Monatsh Chem (2010) 141:945–952
DOI 10.1007/s00706-010-0349-6

ORIGINAL PAPER

Analytical characterization of lichexanthone in lichen: HPLC, UV spectroscopic, and DFT analysis of lichexanthone extracted from *Laurera benguelensis* (Mull. Arg.) Zahlbr.

Zoran S. Marković · Nedeljko T. Manojlović

Received: 27 February 2010 / Accepted: 10 June 2010 / Published online: 30 July 2010

Abstract Lichexanthone, the major pigment present in the extract of *Laurera benguelensis* (Mull. Arg.) Zahlbr., was extracted from lichen, purified, and characterized by high-performance liquid chromatography (HPLC) and ultraviolet (UV) spectroscopy. The geometry of the lichexanthone conformers was optimized at the B3LYP/6-31+G** level of theory. It was found that all conformations have similar energies and that the corresponding lichexanthone radical is planar. In spite of its planarity, there is no significant electron delocalization over the radical. The antioxidant properties of lichexanthone were investigated using the colorimetric assay as Trolox-equivalent antioxidant capacity and at B3LYP/6-31+G** level of theory. Both methods revealed that lichexanthone has weak antioxidant properties. The results confirm the potential of HPLC–UV analysis for taxonomic characterization of lichen species.

Keywords *Laurera benguelensis* · HPLC–UV · Antioxidant activity · Xanthone · DFT

Introduction

It is known that lichen species produce some unique secondary compounds, often in remarkably large quantities [1, 2]. Secondary metabolite data are used more extensively in routine identification of lichens than in any other group of organisms. In an earlier paper, Fourier transform (FT)-Raman and infrared vibrational spectra of some important lichen compounds were characterized. Key biomolecular marker bands have been suggested for spectroscopic identification of atranorin, rhizocarpic acid, fumarprotocetraric acid, calycin, gyrophoric acid, pulvinic dilactone, and usnic acid. FT-Raman spectroscopy has also been used for analytical characterization of the lichen *Parmotrema tinctorum* Del. ex Nyl. [3]. The results confirmed the potential of Raman spectroscopy for taxonomic characterization of lichen species. Xanthones are secondary metabolites commonly occurring in a few higher plant families, fungi, and lichens [4]. They are interesting because of their various pharmacological properties. Most xanthones have phenolic functional groups on a linear tricyclic ring and often exhibit a wide range of biological and pharmacological activities, such as anticancer, anti-inflammatory, antibacterial, and antifungal activities [5, 6]. The biological activities of xanthones are associated with their tricyclic scaffold, but they may vary depending on the nature and/or position of substituents [7]. Xanthones are anticipated to have antioxidant activities such as scavenging of free radicals and superoxide anion, and inhibition of lipid peroxidation. Yoshikawa et al. [8] found that methanolic extracts of *Garcinia mangstana* (GML) hulls showed 2,2-diphenyl-1-picrylhydrazyl (DPPH) radical scavenging activity. α- and γ-mangostins showed antioxidant activity using the ferric thiocyanate method [8, 9].

We report herein a method for extraction, isolation, and identification as well as assessment of antioxidant activity and corresponding bond dissociation enthalpy (BDE) of lichexanthone from the lichen *Laurera benguelensis* (Fig. 1). *Laurera benguelensis* (Mull. Arg.) Zahlbr. is a

Z. S. Marković (✉)
Department of Biochemical and Medical Sciences,
State University of Novi Pazar, 36300 Novi Pazar, Serbia
e-mail: zmarkovic@np.ac.rs

N. T. Manojlović
Department of Pharmacy, Medical Faculty,
University of Kragujevac, 34000 Kragujevac, Serbia
e-mail: ntm@kg.ac.rs

Fig. 1 Specimen of *Laurera benguelensis* (Mull. Arg.) Zahlbr.

tropical microlichen (pyrenomycete) that belongs to the family Trypetheliaceae [10]. Its color is gray to yellow. Lichexanthone (1-hydroxy-3,6-dimethoxy-8-methylxanthen-9-one) is a naturally occurring tetrasubstituted xanthone, which is a constituent in a few higher plant families and lichens [4, 11]. Recent studies have confirmed that lichexanthone and its derivatives possess biological activity, including antimicrobial and cytotoxic activities [12, 13].

There are at least two fundamental and widespread reaction pathways through which xanthones (ArOH) and other phenolic compounds scavenge free radicals: (1) rapid donation of a hydrogen atom to a radical, forming a new radical that is more stable than the initial one [hydrogen atom transfer (HAT) mechanism leading to direct O–H bond breaking]:

$$\mathrm{ArOH} + \mathrm{HO}\cdot \rightarrow \mathrm{ArO}\cdot + \mathrm{HOH}, \quad (1)$$

and (2) the chain-breaking mechanism, by which the primary antioxidant transforms into a radical cation by donating an electron to the free radical present in the system (e.g., lipid or some other radical). This mechanism leads to indirect H-abstraction:

$$\mathrm{ArOH} + \mathrm{HO}\cdot \rightarrow \mathrm{ArOH}^{\cdot +} + \mathrm{OH}^{-} \rightarrow \mathrm{ArO}\cdot + \mathrm{HOH}. \quad (2)$$

The net result of reactions (1) and (2) is the same, and both H atom transfer and electron transfer occur in parallel at different rates. Besides the hydrogen atom transfer mechanism, where the proton and the electron are transferred together, many important biochemical processes proceed via the proton-coupled electron transfer (PCET) mechanism, which occurs when a proton and electron are transferred between different sets of molecular orbitals [14]. Whatever mechanism is involved, the formed radical species ArO· needs to be relatively stable, so that reactions (1) and (2) could be thermodynamically favorable in the sense that it is easier to remove a hydrogen atom from ArOH than from HOH.

For computational investigations of BDE, density functional theory (DFT) and semi-empirical methods are often used [15–17].

The first part of this work aims at HPLC characterization of *L. benguelensis* specimens collected in central Thailand, isolation of the major pigment lichexanthone, its characterization by UV spectroscopy, and determination of its antioxidant capacity. Also, a DFT study on the reactivity of the OH group in lichexanthone and the structural and electronic features of the lichexanthone radical was performed. We present the results of bond order, BDE, highest occupied molecular orbital (HOMO), and Mulliken spin density for lichexanthone. The results of BDE calculations for lichexanthone are presented for the first time. Structure–activity relationships are examined in the light of these results. Particular attention is devoted to the DFT interpretation of the reactivity of the OH group in lichexanthone and the radical formed after H-removal from this molecule. Keto–enol tautomerism before H-abstraction is also discussed to explain the role of the OH group.

Results and discussion

The HPLC chromatogram of the toluene extract of *Laurera benguelensis* is shown in Fig. 2. The t_R value for lichexanthone is 16.59 min. Beside lichexanthone, teloschistin, parietin (anthraquinones), and secalonic acid D (a xanthone derivative) were also identified. Identification of these compounds was achieved by comparison of their t_R values with the standard substances. The UV–Vis absorbance spectral data also corresponded with those in Refs. [18, 19]. Since lichexanthone is the dominant pigment in the extract, this xanthone was isolated from the toluene extract by column chromatography on silica gel.

The geometry of lichexanthone was determined at the B3LYP/6-31+G** level of theory. As the first step, the conformational space of lichexanthone was explored as a function of the torsional angles $\tau 1$ (C2–C3–O–CH_3) and $\tau 2$ (C5–C6–O–CH_3), to determine the preferred relative positions between the CH_3 groups and benzene rings. This minimization procedure yielded a planar conformation ($\tau 1 = \tau 2 = 0°$) as the most stable structure (**1a** in Fig. 3). By removing the constraints on the torsional angles, the conformational absolute minimum was found at $\tau 1 = \tau 2 = 0.0°$, followed by relative minima at: $\tau 1 = 180°$, $\tau 2 = 0.0°$; $\tau 1 = 0°$, $\tau 2 = 180.0°$; and $\tau 1 = 180°$, $\tau 2 = 180.0°$ (**1b**–**1d** in Fig. 3). The energy differences between the absolute and local minima amount to only 0.42, 2.18, and 3.65 kJ/mol. In all structures the hydroxyl group is oriented in such a way as to form a hydrogen bond with the adjacent carbonyl group. Our calculation showed that there is no deviation from planarity in all lichexanthone conformations.

Equilibrium B3LYP/6-31+G** geometrical parameters of the absolute minimum **1a** calculated in vacuum and

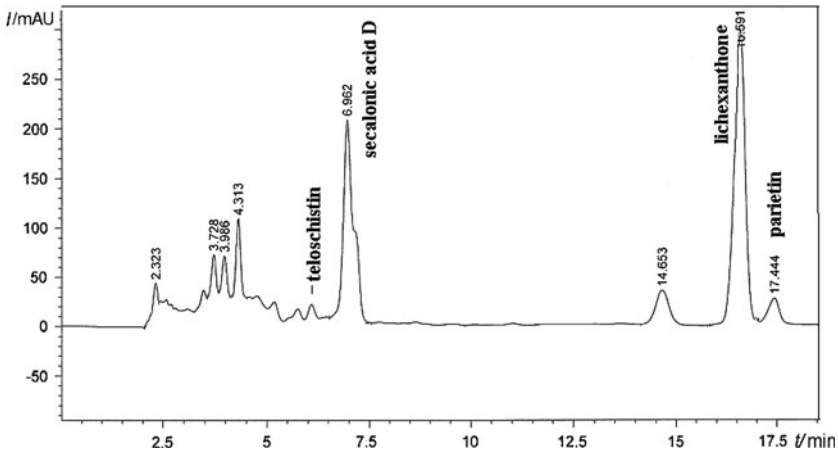

Fig. 2 HPLC chromatogram of a *Laurera benguelensis*

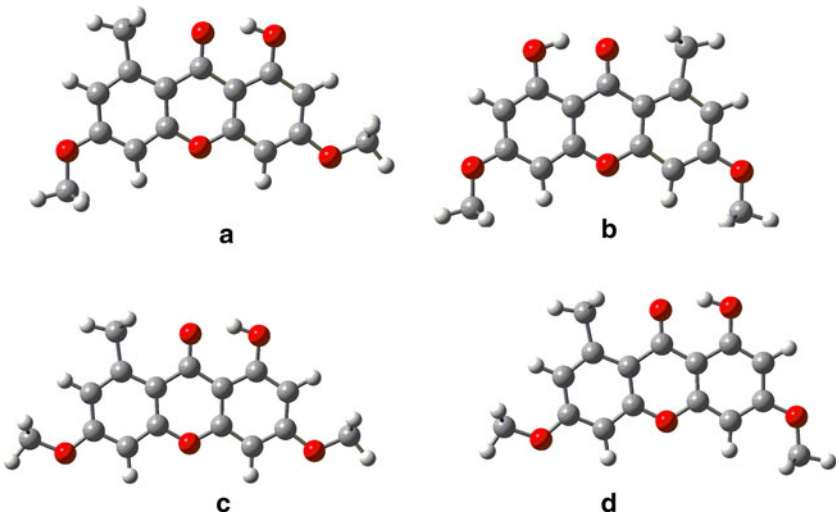

Fig. 3 Optimized geometries of the four conformations of lichexanthone extract

methanol as solvent are reported in Table 1. Table 1 shows that the majority of bonds of **1a** are longer than double bonds but shorter than single bonds. This fact, as well as the planarity of the molecule, indicates a possible extended conjugation and antioxidant properties. This assumption is based on the suggestion of van Acker et al. [20] and Rice-Evans et al. [21], who supposed that the antioxidant properties of flavonoids can be derived just from their good delocalization possibilities. The double bonds in ring C around the carbonyl groups indicate a cross-conjugated system in which delocalization is allowed only between A and C or B and C, but not between rings A and B. This finding is in agreement with the investigation in which biophenol molecules were found to be neither completely planar nor conjugated.

The results of the natural bond orbital (NBO) analysis of **1a** reveal double C9–O bond in carbonyl group, which forms a hydrogen bond with the hydrogen of hydroxyl group (Fig. 3). This hydrogen bond has a stabilizing effect. The conformation lacking this bond is less stable with respect to the absolute minimum by 67.67 kJ/mol. The obtained value is somewhat higher than the corresponding value for emodin [22]. When an electron is removed from the HOMO of a parent molecule, a radical cation species is formed. There is no detailed description of such radical species in literature. The radical cation originating from **1a** is planar and completely conjugated. The hydrogen bond is retained as in the parent molecule, contributing to further stabilization. The calculated ionization potential value (759.56 kJ/mol) of **1a** is higher than the corresponding values for flavonoids [15]. On the basis of the ionization potential value, one can expect lower antioxidant activity for lichexanthone in comparison with flavonoids [23].

To verify the geometry obtained by the DFT method we performed a detailed analysis of experimental and theoretical UV spectra. The experimental and computed UV spectra are presented in Fig. 4, whereas calculated electronic transitions are presented in Table 2. There is generally very satisfactory agreement between the observed and predicted wavenumbers and intensities.

Table 1 DFT bond length values of lichexanthone (**1a**) and its radical (**1–OH**)

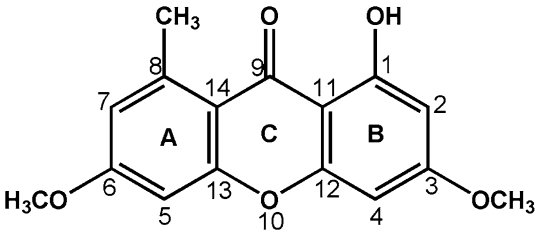

Species bond	Length (nm)		
	1a	**1a** in methanol	**1–OH**
C1–C2	0.139	0.139	0.146
C2–C3	0.140	0.140	0.138
C3–C4	0.140	0.140	0.140
C4–C12	0.138	0.138	0.141
O10–C12	0.136	0.136	0.136
O10–C13	0.136	0.136	0.137
C5–C13	0.139	0.139	0.139
C5–C6	0.139	0.139	0.139
C6–C7	0.140	0.141	0.140
C7–C8	0.138	0.138	0.138
C8–C14	0.143	0.143	0.143
C13–C14	0.141	0.141	0.140
C9–C14	0.146	0.146	0.148
C9–C11	0.145	0.145	0.148
C11–C12	0.140	0.140	0.138
C1–C11	0.142	0.142	0.147
C1–O	0.134	0.134	0.124
C3–O	0.135	0.135	0.135
C6–O	0.135	0.135	0.135
C9–O	0.125	0.126	0.122
C8–C	0.151	0.151	0.151
O3–C	0.142	0.143	0.142
O6–C	0.142	0.143	0.142

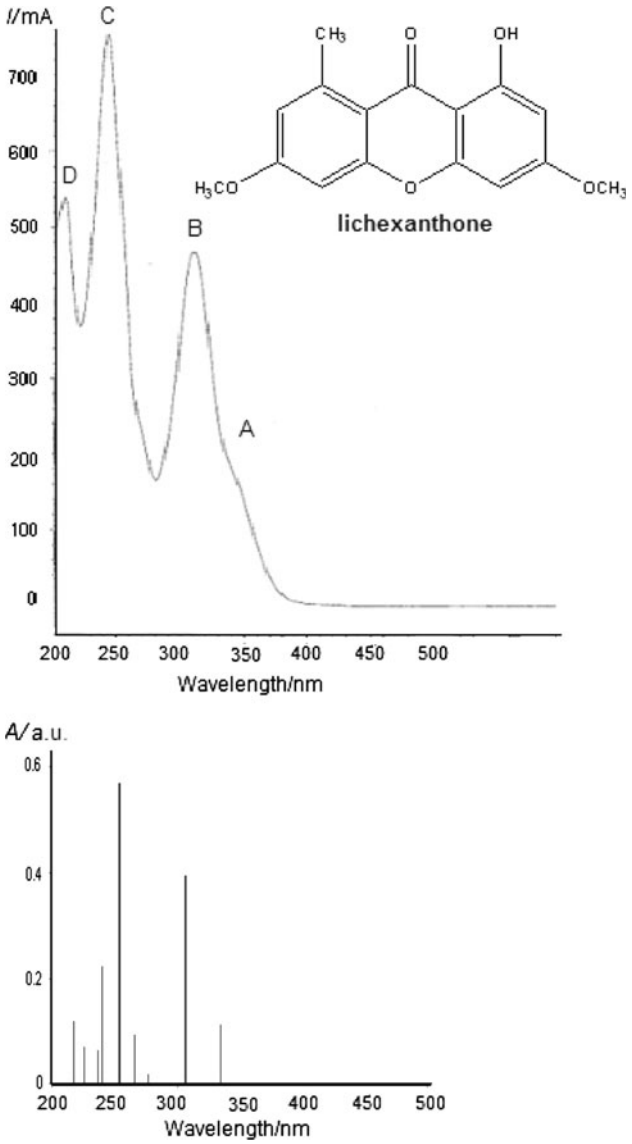

Fig. 4 Experimental (*top*) and calculated (*bottom*) UV spectra for lichexanthone

Table 2 Experimental and calculated electronic transitions for lichexanthone

	Exp.	TD-B3LYP		
	λ (nm)	λ (nm)	f	Leading configurations
A	341	340.9	0.1730	H → L 90%
B	308	306.2	0.3366	H-1 → L 86%
C	244	253.1	0.6004	H → L+1 68%
D	209	234.2	0.2198	H-1 → L+1 47%

λ view number in nm

f oscillator strength

The maximum for band A, a shoulder, whose experimental value is close to 340 nm, is predicted at 340.9 nm. This is essentially a HOMO–lowest unoccupied molecular orbital (LUMO) transition, involving excitation from π to π^*. The shapes of the orbitals shown in Fig. 5 indicate that the transition is associated with significant charge transfer from the phenolic moieties to the carbonyl group, similar to the situation characterizing the color bands in related compounds such as chrysazin and anthralin, and the first strong UV band of the parent 9,10-anthraquinone chromophore [24].

The maximum for the peak B is predicted at 306.2 nm, which is again in excellent agreement with the experimental polarization value of 308 nm. This transition involves excitation from HOMO–1 to LUMO (Fig. 4). On the basis of the shapes of the orbitals it is clear that there is significant charge transfer from aromatic rings to the

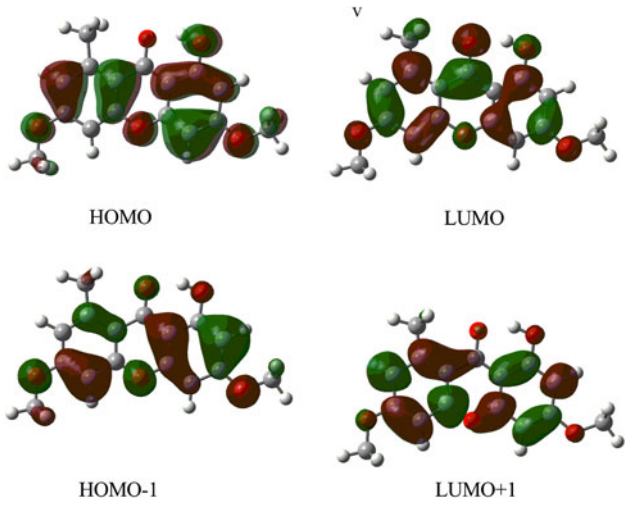

Fig. 5 Selected molecular orbitals for lichexanthone

carbonyl group. The experimental value for peak C, close to 244 nm, is in agreement with the calculated electronic transition of 253.1 nm. In this case there is excitation from HOMO to LUMO+1. The maximum for peak D is close to 209 nm, whereas the value in the predicted spectrum is 234.2 nm. This peak mainly represents excitation from HOMO–1 to LUMO+1.

Antioxidant activity and BDE value of lichexanthone

It is well known that some xanthones are very good antioxidants [8, 9]. For this reason, lichexanthone was screened for its antioxidant potential using the relative ability to scavenge the 2,2′-azino-bis(3-ethylbenzothiazoline-6-sulfonic acid) radical cation ($ABTS^{+}$) generated in the aqueous phase, expressed as Trolox-equivalent antioxidant capacity (TEAC). Lichexanthone was found to have TEAC of 0.022 ± 0.001 mM. This result indicates that lichexanthone has weak antioxidant activity. Since it is well known that there is good correlation between antioxidant activity and BDE values [15, 22], we determined the values of the BDE for the OH group of the lichexanthone. To determine the BDE value for lichexanthone it is necessary to optimize the structure of the corresponding radical. Geometry optimization of the radical was performed starting from the optimized structure of the parent molecule **1a**, removing a hydrogen atom from the OH group at position 1 (Fig. 3). In the discussion, the radical formed by H-removal from the 1–OH group of lichexanthone is called the **1–OH** radical.

The radical retains planarity, like the parent molecule. Inspection of Table 1 allows further comment on the electronic structure of the radical. In the **1–OH** radical, complete delocalization involves only ring A, while ring C is characterized by three double bonds mainly localized on the C1–O carbonyl group, and between the C2–C3 and C11–C12 atoms. A significant difference in comparison with **1a** is the existence of somewhat longer bonds between C1–C2, C4–C12, C9–C14, and C9–C11. On the other hand the bonds between C2–C3, C11–C12, and C9–O are shorter. On the basis of these structural changes it is clear that delocalization between rings C and B is very restricted.

Table 3 presents the BDE value for the radical formed by H-abstraction from **1a**. The BDE value for homolytic cleavage of the O–H bond is higher than those for dissociation of the O–H groups in emodin [22] and especially those in quercetin [15, 16]. This result is in agreement with the experimental TEAC value for lichexanthone (0.022 ± 0.001 mM).

At this stage, we also considered another possible mechanism for explaining the reactivity of the OH group and double bonds in the aromatic rings of lichexanthone: the OH group of lichexanthone can undergo keto–enol tautomerism. The **1–OH** group can form two tautomeric forms with aromatic rings. The hydrogen atom from the **1–OH** group can migrate to position 2 or 11. We calculated the BDE for the formation of the **1–OH** radical by H-abstraction from the C2 and C11 atoms of the keto forms, and obtained the values 303.4 and 271.9 kJ/mol. These low BDE values indicate the relatively high capacity of H-removal from the C2 and especially C11 site in the keto forms. However, it should be noted that the keto forms of lichexanthone are less stable than the enol form, the latter being stabilized by π-conjugation in ring B. The differences in stability between **1a** and C2 and C11 keto forms amount to 113.1 and 144.1 kJ/mol (for instance, in the case of emodin and quercetin, this difference is only about 62.8 and 83.8 kJ/mol [22]). These differences in stability between the enol and keto forms indicate that the contribution of the keto forms can be considered negligible for lichexanthone as a free molecule.

On the other hand, one may presume that, in some enzymatic processes, the stability difference between the two forms is reduced, so that the keto forms become relevant, and then H-abstraction from the C2 or C11 positions can take place easily, thereby contributing to the antioxidant properties. To understand the relationship between electron delocalization and the reactivity of the radical, one can examine the electron distribution in the singly occupied molecular orbital (SOMO). The SOMO of the radical is mainly delocalized over carbonyl groups (Fig. 6). As the SOMO is the α-highest occupied molecular orbital, it does not describe the global electronic behavior of the radical, and its shape is not a reliable indicator for the reactivity of the lichexanthone radical.

Within an unrestricted scheme, the spin density is often considered to be a more realistic parameter and provides a better representation of the reactivity [25]. The more delocalized the spin density in the radical, the more easily the radical is formed and thus the lower the BDE. The

Table 3 Selected calculated energies and molecular orbitals of the lichexanthone molecule (**1a**–**1d**) and its radical in the gas phase

	1a	1b	1c	1d	1–OH
E+ZPE (a.u.)	−994.06067	−994.05998	−994.05984	−994.05928	−993.40367
BDE (kJ/mol)					417.32
HOMO (eV)	−0.225	−0.227	−0.22	−0.227	−0.240
LUMO (eV)	−0.068	−0.0.68	−0.069	−0.069	−0.122
SOMO (eV)					−0.063

BDE bond dissociation enthalpy, *E+ZPE* electronic and zero-point energy, *HOMO* highest occupied molecular orbital, *LUMO* lowest unoccupied molecular orbital, *SOMO* single occupied molecular orbital

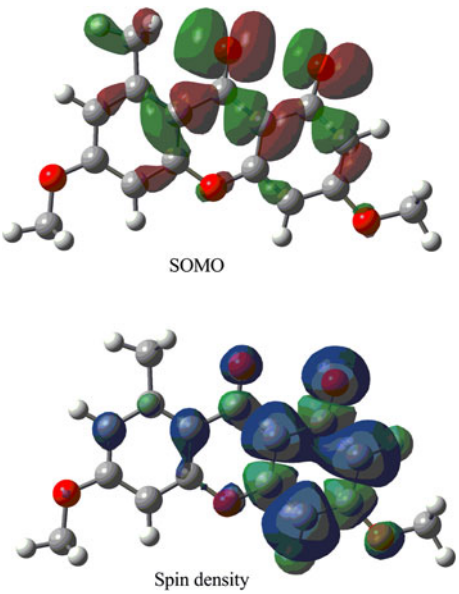

Fig. 6 SOMO and spin density of the **1–OH** radical

importance of the spin density for the description of flavonoids has been pointed out in the recent paper by Leopoldini et al. [15, 16]. We therefore decided to analyze the spin density of the lichexanthone radical. The spin density distribution in the **1–OH** radical indicates the oxygen atom bonded to C1 as the most probable radical center (Fig. 5), followed by the carbons C2, C4, and C11. There is weak delocalization of spin density over rings A and C.

Conclusions

A HPLC–UV method was used for identification of the lichexanthone in *L. benguelensis*. This is of chemotaxonomic importance for *Laurera* sp. due to the fact that very little has been published on the secondary metabolites present in *Laurera* sp. The results confirm the potential of HPLC–UV analysis for precise and rapid identification of this species and other lichexanthone-containing species and their chemotypes. The biological activity of xanthones is associated with their tricyclic scaffold, but they may vary depending on the nature and/or position of substituents. On the basis of the obtained results, it is clear that lichexanthone appears to be a planar tricyclic molecule. In spite of the planarity of the radical structure, there is no significant electronic delocalization between adjacent rings. We suppose that this is one of the main reasons for the higher values of BDE in comparison with those for flavones. Also, the higher BDE value is a consequence of a strong hydrogen bond, because H-removal also implies cleavage of the hydrogen bond. The theoretical results were supported by the experimental (TEAC) value of ABTS. It was found that the enol form is the most stable tautomer in the free molecule; the keto forms, which possess much lower BDEs for H-abstraction on the C2 or C11 atoms, might play a significant role in real systems, depending on the molecular environment of lichexanthone and the oxidative system acting on the molecule.

Experimental

Lichen material was collected from Kanchanaburi Province (10 km south of the Erawan National Park) in Thailand during July 2006. The studied lichen was identified by Prof. Dr. Boonpagob, Department of Biology, Faculty of Science, Ramkhamhaeng University, Bangkok, Thailand as *Laurera benguelensis* (Mull. Arg.) Zahlbr. (voucher specimen RU-22160).

High-performance liquid chromatography analysis

HPLC analysis was carried out on an Agilent 1200 Series HPLC instrument with C18 column (C18; 25 cm × 4.6 mm, 10 m) and a UV spectrophotometric detector with methanol–water–phosphoric acid (80:20:0.9, v/v/v) solvent. Methanol was of HPLC grade and was purchased from Merck (Darmstadt, Germany). Phosphoric acid was analytical-grade reagent. Deionized water used throughout the experiments was generated by a Milli-Q academic water purification system (Milford, MA, USA). The sample

injection volume was 10 mm^3. The flow rate was 1.0 cm^3/min. The lichexanthone was identified by comparison of its retention time and absorption spectrum (200–600 nm) and also compared with literature data [12].

Preparation of lichen extract

The lichen material was air-dried at room temperature (26 °C) for 1 week, after which it was ground to a uniform powder. The toluene extract was prepared by soaking 10 g dry powdered lichen material in 100 cm^3 toluene at room temperature for 48 h. The extract was filtered after 48 h through a Whatman no. 42 (125 mm) filter paper and concentrated using a rotary evaporator. The percentage yield of the extract was 5.12% w/w.

Isolation of lichexanthone

Toluene extract (100 mg) was fractionated on a silica gel column. The column was eluted with toluene. The first eluted fraction of the *L. benguelensis* extract contains lichexanthone (25 mg), which was further purified by co-chromatography and preparative layer chromatography and used for structure identification and antioxidant studies. Lichexanthone was identified by its m.p. of 188–190 °C (188–190 °C [12]) and its spectroscopic properties [12]. UV (methanol): $\lambda = 208$ (71%), 243 (100%), 309 (65%), 341 (sh) nm.

Antioxidant activity

ABTS and Trolox (6-hydroxy-2,5,7,8-tetramethylchromane-2-carboxylic acid) were obtained from Fluka (Switzerland). The total antioxidant activity of lichexanthone was determined by colorimetric assay as Trolox-equivalent antioxidant capacity (TEAC). The stable ABTS radical monocation ($ABTS^+$) was generated by incubation of 7 mM ABTS with 2.5 mM potassium persulfate in the dark at room temperature for 12–16 h before use. The $ABTS^+$ solution was diluted immediately prior to assay to absorbance of 0.70 ± 0.02 at 734 nm. Diluted $ABTS^+$ solution (0.5 cm^3) was placed in a quartz cuvette to record initial absorbance. Then, various concentrations of lichexanthone or Trolox were added to each cuvette and mixed by inversion, and absorbance at 60 s after addition was exactly read. Parallel blanks were performed in each assay with the appropriate solvent alone. Decolorization of blue–green color of ABTS radical cation was proportional to their antioxidant activity. Percentage inhibition compared with initial absorbance after 60 s was plotted as a function of sample or Trolox concentration. TEAC value was expressed as the ratio of sample and Trolox slope (a_{sample}/a_{Trolox}). Each assay was carried out in triplicate [26].

Computational method

All calculations were performed using the Gaussian03 software package [27]. The gas-phase minimum-energy equilibrium geometry of lichexanthone was calculated using the B3LYP method [28] and 6-31+G(d,p) basis set [27]. Four minima corresponding to different in-plane conformations of the OCH_3 groups at positions 3 and 6 (Table 1) were localized. An energy difference between the most stable and most unstable of 3.8 kJ/mol was found. The geometries thus obtained were verified to be minima on the potential energy surface by normal-mode analysis; no imaginary frequencies were obtained. The most stable molecular conformation is shown in Fig. 3, and the computed bond lengths are listed in Table 1. Transitions to the lowest excited singlet electronic states of lichexanthone were computed using the TD-B3LYP procedure [29, 30] with the 6-31+G(d,p) basis set [28]. The influence of methyl alcohol as solvent upon the electronic transitions was approximated by the polarized continuum model (PCM) [31, 32]. This level of approximation is similar to that recommended by Perpète and coworkers for anthraquinone dyes (level "M–C") [33], except for inclusion of diffuse basis functions in the present TD calculation. Essentially similar electronic transitions were predicted for the four conformations mentioned above. The computed electronic transitions for the most stable conformation (Fig. 3) are presented in Table 3. UV spectral analysis was performed using ChemCraft 1.5 [34].

The obtained zero-point energies were used to correct all energetic terms using the recommended scaling factors [35]. Natural bond orbital (NBO) [36] analysis was performed for all structures. The bond dissociation enthalpy (BDE) for lichexanthone was calculated using the following equation:

$$\mathrm{BDE} = H_{\mathrm{LOH}} - H_{\mathrm{LO}\cdot} - H_{\mathrm{H}\cdot},$$

where H_{LOH}, $H_{\mathrm{LO}\cdot}$, and $H_{\mathrm{H}\cdot}$ represent the enthalpies of lichexanthone, lichexanthone radical, and hydrogen atom, respectively. The ionization potential (IP) was obtained as the energy difference between the LOH and $\mathrm{LOH}^+\cdot$ species.

Acknowledgments The authors acknowledge financial support by the Ministry of Science and Environmental of Republic of Serbia (grant no. 142025).

References

1. Yamamoto Y (1991) Production of Lichen Substances. In: Komamine A, Misawa M, DiCosmo F (eds) Plant cell culture in Japan. CMC Co., Tokyo
2. Langcake P, Pryce RJ (1976) Physiol Plant Pathol 9:77
3. Oliveira LFC, Pinto PCC, Marcelli MP, Dos Santos HF, Edwards GMH (2009) J Mol Struct 920:128

4. Vieira LMM, Kijjoa A (2005) Curr Med Chem 12:2413
5. Akao Y, Nakagawa Y, Iinuma M, Nozawa Y (2008) Int J Mol Sci 9:355
6. Chen LG, Yang LL, Wang CC (2008) Food Chem Toxicol 46:688
7. Pinto MMM, Souza ME, Nascimento MSJ (2005) Curr Med Chem 12:2517
8. Yoshikawa M, Harada E, Miki A, Tsukamoto K, Si Qian L, Yamahara J, Murakami N (1994) Yakugaku Zasshi 114:129
9. Fan C, Su J (1997) J Chin Agric Chem Soc 35:540
10. Vongshewarat K, McCarthy PM, Mongkolsuk P, Boonpagob K (1999) Mycotaxon 70:227
11. El-Seedi HR, Hazell AC, Torssell KBG (1994) Phytochemistry 35:1297
12. Micheletti AC, Beatriz A, Lima DP, Honda NK, Pessoa C, Odorico de Moraes M, Lotufo LV, Magalhães HIF, Carvalho NCP (2009) Quím Nova 32:12
13. Wansi JD, Wandji J, Waffo AFK, Ngeufa HE, Ndom JC, Fotso S, Maskey RP, Dieudonné N, Fomum TZ, Laatsch H (2006) Phytochemistry 67:475
14. Mayer MJ (2004) Annu Rev Phys Chem 55:363
15. Leopoldini M, Pitarch IP, Russo N, Toscano M (2004) J Phys Chem A 108:92
16. Leopoldini M, Marino T, Russo N, Toscano M (2004) Theor Chem Acc 111:210
17. Trouillas P, Fagnère C, Lazzaroni R, Calliste AC, Marfak A, Duroux LJ (2004) Food Chem 88:571
18. Huneck S, Yoshimura I (1996) Identification of Lichen Substances. Springer, Berlin
19. Manojlovic TN, Solujic S, Sukdolak S (2002) Lichenologist 3:83
20. van Acker SABE, Groot MJ, van der Vijgh WJF, Tromp MNJL, den Kelder GF, van der Vijgh EJF, Bast A (1996) Chem Res Toxicol 9:1305
21. Rice-Evans CA, Miller NJ, Paganga G (1996) 20:933
22. Markovic SZ, Manojlovic TN (2009) Monatsh Chem 140:1311
23. Cai YZ, Sun M, Xing J, Luo Q, Corke H (2006) Life Sci 78:2872
24. Møller S, Andersen KB, Spanget-Larsen J, Yaluk J (1988) Chem Phys Lett 291:51
25. Szabo A, Ostlund NS (1982) Modern quantum chemistry: introduction to advanced electronic structure theory. Dover, New York
26. Cai YZ, Luo Q, Sun M, Corke H (2004) Life Sci 74:2157
27. Frisch MJ, Trucks GW, Schlegel HB, Scuseria GE, Robb MA, Cheeseman JR, Zakrzewski VG, Montgomery JA Jr, Stratmann RE, Burant JC, Dapprich S, Millam JM, Daniels AD, Kudin KN, Strain MC, Farkas O, Tomasi J, Barone V, Cossi M, Cammi R, Mennucci B, Pomelli C, Adamo C, Clifford S, Ochterski J, Petersson GA, Ayala PY, Cui Q, Morokuma K, Malick AD, Rabuck KD, Raghavachari K, Foresman JB, Cioslowski J, Ortiz JV, Baboul AG, Stefanov BB, Liu G, Liashenko A, Piskorz P, Komaromi I, Gomperts R, Martin RL, Fox DJ, Keith T, Al-Laham MA, Peng CY, Nanayakkara A, Challacombe M, Gill PMW, Johnson B, Chen W, Wong MW, Andres JL, Gonzalez C, Head-Gordon M, Replogle ES, Pople JA (2003) Gaussian 03, Revision E.01-SMP. Gaussian Inc., Pittsburgh
28. Becke AD (1992) J Chem Phys 97:9173
29. Becke AD (1993) J Chem Phys 98:5648
30. Lee C, Yang W, Parr RG (1988) Phys Rev B 37:785
31. Miertuš S, Scrocco S, Tomasi J (1981) Chem Phys 55:117
32. Tomasi J, Mennucci B, Cammi R (2005) Chem Rev 105:2999
33. Jacquemin D, Assfeld X, Preat J, Perpète EA (2007) Mol Phys 105:325
34. Zhurko GA, Chemcraft graphical program for working with quantum chemistry results
35. Merrick JP, Moran DL (2007) J Phys Chem 11:11683
36. Foster JP, Weinhold F (1980) J Am Chem Soc 102:7211